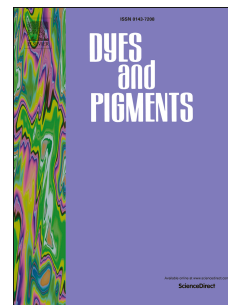


Journal Pre-proof

Construction of red-emitting iminocoumarin-based fluorescent borate complexes with a large Stokes shift

Xiaojie Ren, Man Guo, Junyi Gong, Yun Zhang, Lei Yang, Xingjiang Liu, Xiangzhi Song



PII: S0143-7208(19)31867-4

DOI: <https://doi.org/10.1016/j.dyepig.2019.108007>

Reference: DYPI 108007

To appear in: *Dyes and Pigments*

Received Date: 6 August 2019

Revised Date: 27 October 2019

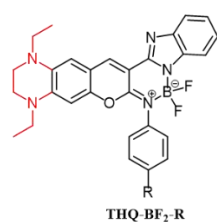
Accepted Date: 28 October 2019

Please cite this article as: Ren X, Guo M, Gong J, Zhang Y, Yang L, Liu X, Song X, Construction of red-emitting iminocoumarin-based fluorescent borate complexes with a large Stokes shift, *Dyes and Pigments* (2019), doi: <https://doi.org/10.1016/j.dyepig.2019.108007>.

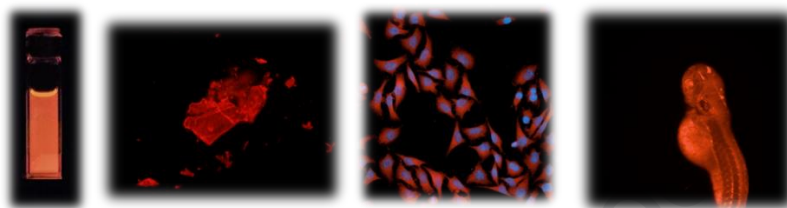
This is a PDF file of an article that has undergone enhancements after acceptance, such as the addition of a cover page and metadata, and formatting for readability, but it is not yet the definitive version of record. This version will undergo additional copyediting, typesetting and review before it is published in its final form, but we are providing this version to give early visibility of the article. Please note that, during the production process, errors may be discovered which could affect the content, and all legal disclaimers that apply to the journal pertain.

© 2019 Published by Elsevier Ltd.

Graphical Abstract



- ♪ Red/NIR emission
- ♪ Large Stokes shift
- ♪ High fluorescent quantum yield
- ♪ Good staining ability in cells and zebrafish



A series of red-emitting iminocoumarin-based borate dyes with tetra-hydro-quinoxaline (THQ) moiety as the electron donor, **THQ-BF₂-R**, were developed. These borate dyes exhibited fairly high fluorescent quantum yields, large Stokes shifts and long-wavelength emissions. These dyes could be potentially used as staining agents for biological applications.

Construction of Red-emitting Iminocoumarin-based Fluorescent Borate Complexes with A Large Stokes Shift

Xiaojie Ren,^a Man Guo,^a Junyi Gong,^a Yun Zhang,^a Lei Yang,^a Xingjiang Liu^{b,*} and Xiangzhi Song^{a, c, *}

^a College of Chemistry & Chemical Engineering, Central South University, Changsha, Hunan Province, China, 410083.

* Corresponding author. Email: song@rowland.harvard.edu. (Xiangzhi Song)

^b College of Chemistry & Chemical Engineering, Zhengzhou University, Zhengzhou, Henan, Province, China, 450001.

* Corresponding author. Email: xingjiangliu@zzu.edu.cn (Xingjiang Liu).

^c Key Laboratory of Hunan Province for Water Environment and Agriculture Product Safety, Changsha, Hunan Province, China, 410083

Abstract: Tetra-hydro-quinoxaline (THQ) moiety was used as the electron donor in the construction of a series of red-emitting iminocoumarin-based borate dyes with good fluorescent quantum yields, large Stokes shifts and long-wavelength emissions. These dyes could stain cells and image zebrafish with good performance.

Key words: borate, tetra-hydro-quinoxaline, Stokes shift, red-emitting, fluorescent dyes

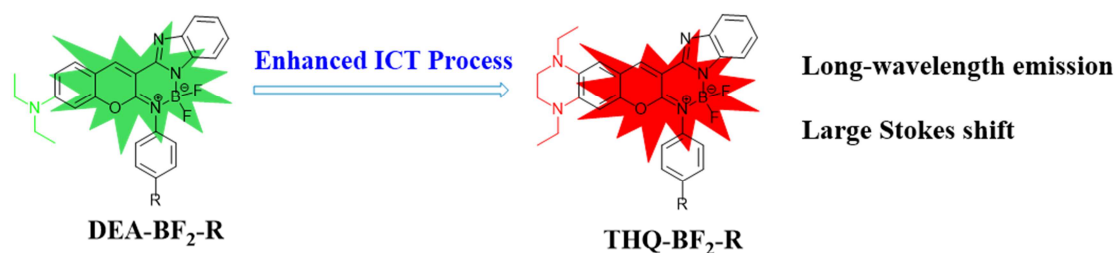
1. Introduction

4,4-Difluoro-4-bora-3a,4a-diaza-s-indacene (**BODIPY**) have been widely utilized as biological sensing agents[1-5], photodynamic therapeutic agents[6], laser dyes[7], and optoelectronic materials[8] because of their advantageous photo-physical properties such as good photo-stability, high molar absorption coefficient and high fluorescence quantum yield.[9, 10] While being valuable, most of **BODIPY** dyes suffer from very small Stokes shifts (usually < 30 nm), which usually causes serious self-absorption and thereby leads to measurement errors in fluorescence sensing. Moreover, most of **BODIPY** dyes exhibited fluorescence quenching in aggregation form and/or solid state due to the strong intermolecular π - π stacking.[11, 12]

In principle, asymmetrical donor–acceptor (D-A) type fluorescent dyes display larger Stokes shift and longer emission than their symmetrical analogues.[13, 14] In 2013, Ziessel’s group[15] pioneered a new kind of iminocoumarin-based borate complexes, Borico dyes (**DEA-BF₂-R**), having asymmetrical structure with diethylamino group as the electron donor and “N-BF₂-N” moiety as the electron acceptor (Scheme 1). These dyes possess high fluorescent quantum yields in solution (up to 80%). However, their emissions are in relatively short wavelength spectral regions (blue and green) and their Stokes shifts are still small (< 50 nm), which affect their applications for bioimaging and sensing due to the weak tissue penetration ability and strong background interference.[16-21]

In the design of fluorescent dyes and fluorescent probes, introducing strong electron donors such tetra-hydro-quinoxaline group (THQ) and julolidine moiety (Julo) has been proved to be an efficient strategy to lengthen emission wavelengths as well as Stokes shifts due to the enhanced ICT process.[22-26] Besides, fluorescent dyes with such electron donors can retain a relatively high fluorescent quantum yield because the rigid structure of THQ and Julo moieties can effectively prohibit the formation of TICT (twisted intramolecular charge transfer) state.[27-29]

In this work, we used tetra-hydro-quinoxaline group (THQ) to replace diethylamino group (DEA) in **DEA-BF₂-R** dyes to obtain a series of new iminocoumarin-based borate complexes, **THQ-BF₂-R**, which are expected to exhibit long-wavelength emission and large Stokes shift, as shown in Scheme 1. In addition, we also used julolidine moiety (Julo) to replace diethylamino group (DEA) in **DEA-BF₂-R** to prepare another rigid borate complexes, **Julo-BF₂-R**.



Scheme 1. Tuning the optical properties of iminocoumarin-based borate dyes by enhancing the electron-donating ability of donors.

2. Experimental

2.1 General methods

All reagents were purchased from commercial suppliers without further purification. The absorption spectra were detected using an Agilent UV-2450 spectrophotometer and the corrected fluorescence spectra were recorded on a Hitachi F-7000 spectrophotometer. The fluorescent lifetimes were determined on a Pico Quant GmbH Fluo Time 100 lifetime spectrometer. The absolute fluorescent quantum yields for the solid samples were detected on a Hamamatsu Quantarus-QY C11347. The fluorescent quantum yields in solution were measured on a Hitachi F-7000 spectrophotometer using a standard reference and calculated from the following equation:

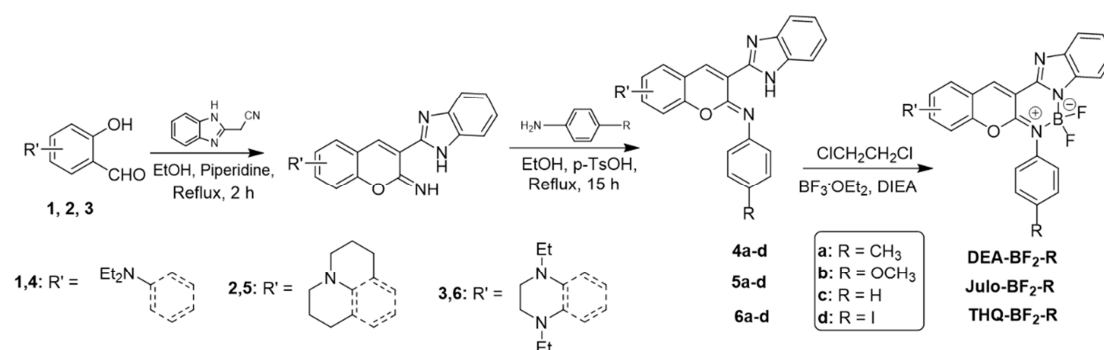
$$\Phi_u = \Phi_s \frac{F_u}{F_s} \frac{A_s}{A_u} \frac{n_u^2}{n_s^2}$$

Φ denotes the fluorescent quantum yield; F means the integral intensity of fluorescence, A refers to the absorbance at the excitation wavelength and n is the refraction index of solvents. u and s represent the testing sample and the standard sample, respectively.

^1H NMR and ^{13}C NMR were obtained on Bruker 400/500 spectrometers (using TMS as an internal standard). Mass spectra were measured using a Bruker ESI-TOF-Q spectrometer. Fluorescence photos of solid samples were obtained on an Olympus IX83 inverted microscope. Fluorescence imaging experiments in living cells and zebrafish were performed on an Opera Phenix/Operetta CLS from PerkinElmer, Inc. All the tests were conducted at room temperature.

2.2 Synthesis

These dyes were prepared according to the procedure shown in Scheme 2. Firstly, aminosalicylaldehydes reacted with 2-cyanomethylbenzimidazole in ethanol to afford iminocoumarins,[30] which condensed with substituted anilines to give compounds **4a-d**, **5a-d** and **6a-d**. Without further purification, compounds **4a-d**, **5a-d** and **6a-d** were treated with $\text{BF}_3 \cdot \text{OEt}_2$ to yield the borate complexes **DEA-BF₂-R**, **Julo-BF₂-R** and **THQ-BF₂-R**. All these new compounds were fully characterized by NMR and HRMS analysis.



Scheme 2. General synthetic procedure of borate dyes.

2.2.1 General procedure for the synthesis of DEA-BF₂-R

Dyes **DEA-BF₂-CH₃**, **DEA-BF₂-OCH₃**, **DEA-BF₂-H** were prepared according to the literature methods.[15]

Synthesis of DEA-BF₂-I: Under an argon atmosphere, a solution of 4-diethylaminosalicylaldehyde (1 mmol) (compound **1**), 2-cyanomethylbenzimidazole (1.1 mmol) and piperidine (15 μ L) in ethanol was stirred for 2 hours. Then, the reaction solution was diluted with 10 mL anhydrous ethanol and *p*-toluenesulfonic acid (*p*-TsOH, 5 mg) and 4-iodoaniline (2 mmol) were added. After stirring for 15 hours, the mixture was cooled down and the solvent was removed and the residue was purified by column chromatograph (CH₂Cl₂: C₂H₅OH 100:1) to afford compound **4d**.

Without further purification, compound **4d** was dissolved in 1,2-dichloroethane (10 mL), then N, N-di-isopropyl-amine (100 μ L) and BF₃•OEt₂ (100 μ L) were added. The mixture was refluxed for 2 hours under an argon atmosphere. After cooling to room temperature, the reaction was quenched with saturated aqueous NaHCO₃ solution and extracted with CH₂Cl₂ three times (3 x 30 mL). The organic layers were collected, combined and dried over anhydrous Na₂SO₄ for 2 hours. After the removal of solvent, the obtained residue was purified by silica gel column chromatograph twice (CH₂Cl₂: C₂H₅OH = 100:1) to give a solid, which was then recrystallized in the mixture of DCM: PE (5:1) to give pure **DEA-BF₂-I** as a red powder. Yield 6.8%.

¹H NMR (400 MHz, CDCl₃) δ 9.09 (s, 1H), 7.97-7.86 (m, 2H), 7.71 (t, *J* = 8.5 Hz, 1H), 7.66 (s, 1H), 7.56-7.47 (m, 1H), 7.31 (t, *J* = 10.5 Hz, 2H), 7.25-7.11 (m, 2H), 6.71 (dd, *J* = 9.1, 2.4 Hz, 1H), 6.19 (d, *J* = 2.1 Hz, 1H), 3.43 (q, *J* = 7.1 Hz, 4H), 1.23 (t, *J* = 7.1 Hz, 6H). ¹³C NMR (100 MHz, CDCl₃) δ 159, 154.5, 152.9, 145.3, 143.7, 140.6, 138.6, 136.56, 135.9, 131.4, 129.0, 122.8, 117.5, 113.9, 112.2, 109.3, 104.3, 96.42, 93.8, 45.16, 12.5. HRMS (ESI) *m/z* [C₂₆H₂₂BF₂IN₄O+H]⁺ calcd.: 582.0899, found: 583.0983.

2.2.2 General procedure for the synthesis of Julo-BF₂-R

Dissolved compound **2** (julolidine-salicylaldehyde, 1 mmol) and 2-cyanomethyl-benzimidazole (1.1 mmol) in 10 mL anhydrous acetonitrile, then 15 μ L piperidine was added into above solution. The obtained solution was refluxed under argon atmosphere for 2 hours to precipitate a yellowish-brown solid. To the above reaction solution were added 10 mL anhydrous acetonitrile, 5 mg *p*-TsOH and 2 mmol *p*-R-aniline (R = -CH₃, -OCH₃, -H, -I). Then the reaction mixture was refluxed under an argon atmosphere until the solid disappeared (about 15 hours). Cooling the reaction mixture to room temperature, and the solution was evaporated in vacuum. The residue was purified by silica gel column chromatograph (CH₂Cl₂: C₂H₅OH from 100:1 to 50:1) to give crude products **5a/5b/5c/5d** as

red solid, which were used for the next reactions without further purification.

The respective **5a/5b/5c/5d** was dissolved in 20 mL 1,2-dichloroethane and 100 μ L N,N-di-isopropyl-amine and 100 μ L $\text{BF}_3 \cdot \text{OEt}_2$ were added. The mixture was stirred at 80 °C under an argon atmosphere until the dark-red solution turned into yellow-green (about 2 hours). After cooling to room temperature, the reaction was quenched with saturated aqueous NaHCO_3 solution and the reaction mixture was extracted with CH_2Cl_2 three times (3 x 30 ml). The organic layers were collected and dried over anhydrous Na_2SO_4 for 2 hours. The solvent was removed by distillation and the residue was purified with column chromatograph to yield a red solid, which was further purified by recrystallization from the mixture DCM: PE (5: 1) to yield the pure products.

Julo-BF₂-CH₃: Silica gel, CH_2Cl_2 : $\text{C}_2\text{H}_5\text{OH}$ (from 100: 0 to 100: 1). Yield: 10.3%. ¹H NMR (400 MHz, CDCl_3) δ 8.92 (d, $J = 55.3$ Hz, 1H), 7.72 (dd, $J = 15.2, 7.6$ Hz, 2H), 7.46 (d, $J = 8.2$ Hz, 2H), 7.38 (d, $J = 8.2$ Hz, 2H), 7.27-7.17 (m, 2H), 7.09 (s, 1H), 3.32-3.19 (m, 4H), 2.75 (t, $J = 6.1$ Hz, 2H), 2.49 (s, 3H), 2.22 (dd, $J = 13.1, 6.7$ Hz, 2H), 1.98-1.87 (m, 2H), 1.87-1.75 (m, 2H). ¹³C NMR (100 MHz, CDCl_3) δ 149.5, 148.9, 145.6, 140.7, 137.9, 135.7, 134.0, 129.91, 127.4, 126.6, 123.2, 122.9, 122.0, 116.9, 114.1, 109.2, 105.9, 50.4, 49.8, 27.3, 21.3, 20.7, 19.7, 19.0. HRMS (ESI) m/z [$\text{C}_{29}\text{H}_{25}\text{BF}_2\text{N}_4\text{O}+\text{H}$]⁺ calcd.: 495.2168, found: 495.2100.

Julo-BF₂-OCH₃: Silica gel, CH_2Cl_2 : $\text{C}_2\text{H}_5\text{OH}$ (from 100: 0 to 100: 1). Yield: 10.8%. ¹H NMR (500 MHz, CDCl_3) δ 7.74 (t, $J = 8.6$ Hz, 1H), 7.48 (d, $J = 8.7$ Hz, 1H), 7.24 (dd, $J = 16.9, 8.9$ Hz, 1H), 7.09 (d, $J = 8.6$ Hz, 1H), 3.92 (s, 1H), 3.36-3.30 (m, 1H), 3.30-3.22 (m, 1H), 2.80 (t, $J = 6.1$ Hz, 1H), 2.27 (t, $J = 6.4$ Hz, 1H), 2.00-1.93 (m, 1H), 1.88-1.81 (m, 1H). ¹³C NMR (100 MHz, CDCl_3) δ 159.15, 149.40, 148.64, 146.27, 139.70, 136.06, 129.53, 128.00, 127.16, 122.54, 122.34, 121.95, 117.37, 114.49, 113.80, 109.21, 105.75, 77.54, 77.08, 76.76, 55.57, 50.26, 49.90, 49.38, 49.16, 48.95, 27.31, 20.67, 19.68, 19.06. HRMS (ESI) m/z [$\text{C}_{29}\text{H}_{25}\text{BF}_2\text{N}_4\text{O}_2+\text{H}$]⁺ calcd.: 511.2117, found: 511.2025.

Julo-BF₂-H: Silica gel, CH_2Cl_2 : $\text{C}_2\text{H}_5\text{OH}$ (from 100: 0 to 50: 1). Yield: 10.5%. ¹H NMR (500 MHz, CDCl_3) δ 8.84 (s, 1H), 7.72 (dd, $J = 12.1, 7.8$ Hz, 2H), 7.59 (d, $J = 4.4$ Hz, 4H), 7.49 (dt, $J = 8.7, 4.2$ Hz, 1H), 7.22 (dt, $J = 20.5, 6.9$ Hz, 2H), 7.07 (s, 1H), 3.33-3.27 (m, 2H), 3.27-3.20 (m, 2H), 2.78 (t, $J = 6.2$ Hz, 2H), 2.18 (t, $J = 6.4$ Hz, 2H), 1.99-1.92 (m, 2H), 1.80 (dd, $J = 11.7, 6.1$ Hz, 2H). ¹³C NMR (100 MHz, CDCl_3) δ 149.3, 148.4, 146.2, 144.7, 139.5, 137.0, 136.3, 129.2, 128.0, 127.0, 122.6, 117.6, 113.7, 109.1, 105.7, 103.5, 50.2, 49.6, 27.3, 20.7, 19.6, 18.9. HRMS (ESI) m/z [$\text{C}_{29}\text{H}_{25}\text{BF}_2\text{N}_4\text{O}_2+\text{H}$]⁺ calcd.: 511.2117, found: 511.2025.

Julo-BF₂-I: Silica gel, CH_2Cl_2 : $\text{C}_2\text{H}_5\text{OH}$ (from 100: 0 to 25: 1). Yield: 10%. ¹H NMR (500 MHz, CDCl_3) δ 9.06 (s, 1H), 7.91 (d, $J = 8.4$ Hz, 2H), 7.75 (d, $J = 7.8$ Hz, 1H), 7.72 (d, $J = 7.8$ Hz, 1H), 7.35 (d, $J = 8.3$ Hz, 2H), 7.25 (dd, $J = 13.4, 5.9$ Hz, 2H), 7.16 (s, 1H), 3.41-3.35 (m, 2H), 3.35-3.28 (m, 2H), 2.80 (t, $J = 6.1$ Hz, 2H), 2.26 (t, $J = 6.3$ Hz, 2H), 1.99 (dd, $J = 11.3, 5.8$ Hz, 2H), 1.88 (dd, $J = 11.9, 6.3$ Hz, 3H). ¹³C NMR (100 MHz, CDCl_3) δ 153.48, 144.17, 142.38, 133.02, 132.71, 131.31, 126.79, 126.54, 121.04, 117.68, 113.44, 109.64, 96.87, 81.48, 81.16,

80.84, 54.31, 53.73, 53.35, 53.14, 52.93, 52.71, 52.50, 52.28, 52.07, 31.26, 24.52, 23.51, 22.99.
 HRMS (ESI) m/z $[C_{28}H_{22}BF_2IN_4O+H]^+$ calcd.: 607.0978, found: 607.0871.

2.2.3 General procedure for the synthesis of THQ-BF₂-R

To a solution of compound **3** (2,4-diethylamino-1,2,3,4-tetrahydro-quinoxaline, 1 mmol) and 2-cyanomethyl-benzimidazole (1.1 mmol) in 5 ml anhydrous ethanol was added 15 μ L piperidine. The mixture was stirred for 2 hours at 80 °C under an argon atmosphere. 10 mL anhydrous ethanol was added to dilute the reaction mixture, then 5 mg *p*-TsOH and 2 mmol *p*-R-aniline (R = -CH₃, -OCH₃, -H, -I) were added. The resulting reaction solution was refluxed for 15 hours. After cooling to room temperature, the solvent was distilled in vacuum. The obtained residue was purified by column chromatography using CH₂Cl₂: C₂H₅OH (100: 1) as the eluent to yield a red solid, which was used for the next step without further purification.

A solution of **6a/6b/6c/6d**, N, N-di-isopropyl-amine (100 μ L) and BF₃•OEt₂ (100 μ L) in 1,2-dichloroethane (20 mL) was refluxed for 2 hours under an argon atmosphere. After cooling to room temperature, dichloromethane (20 mL) was added into the reaction mixture, which was then quenched with saturated aqueous NaHCO₃ solution and extracted with CH₂Cl₂ three times (3 x 30 ml). The organic layers were combined and dried over anhydrous Na₂SO₄ for 2 hours. After the removal of solvent, the residue was purified by column chromatography twice using CH₂Cl₂: C₂H₅OH (from 100: 1 to 50: 1) as the eluent to give the pure products.

THQ-BF₂-CH₃: Dark red solid. Yield: 6.16%. ¹H NMR (400 MHz, CDCl₃) δ 9.12 (s, 1H), 7.81 (dd, J = 10.7, 4.3 Hz, 2H), 7.41 (d, J = 8.6 Hz, 2H), 7.38 (d, J = 8.5 Hz, 2H), 7.35-7.29 (m, 2H), 6.65 (s, 1H), 6.25 (s, 1H), 3.63-3.53 (m, 2H), 3.42 (q, J = 7.1 Hz, 4H), 3.34-3.25 (m, 2H), 2.50 (s, 3H), 1.32-1.11 (m, 5H). ¹³C NMR (100 MHz, CDCl₃) δ 142.95, 141.76, 138.23, 133.88, 130.70, 126.64, 126.42, 121.25, 117.78, 114.66, 110.29, 98.93, 81.42, 81.10, 80.78, 53.49, 53.28, 53.07, 52.85, 52.64, 52.43, 52.21, 51.25, 50.16, 49.37, 47.99, 25.04, 14.55, 13.50. HRMS (ESI) m/z $[C_{29}H_{29}BF_2N_5O+H]^+$ calcd.: 512.2433, found: 512.2549.

THQ-BF₂-OCH₃: Dark red solid. Yield: 6.35%. ¹H NMR (400 MHz, CDCl₃) δ 9.69 (s, 1H), 7.93 (d, J = 7.5 Hz, 1H), 7.84 (d, J = 7.6 Hz, 1H), 7.55 (d, J = 9.0 Hz, 1H), 7.41 (p, J = 7.1 Hz, 3H), 7.18-7.03 (m, 2H), 6.78 (s, 2H), 6.26 (s, 1H), 3.94 (s, 3H), 3.71-3.56 (m, 2H), 3.45 (dq, J = 14.4, 7.2 Hz, 4H), 3.36-3.25 (m, 2H), 1.26 (dd, J = 12.3, 5.1 Hz, 6H). ¹³C NMR (100 MHz, CDCl₃) δ 163.19, 154.22, 148.98, 145.07, 144.91, 144.68, 138.34, 132.97, 132.00, 128.77, 128.17, 123.30, 121.08, 118.97, 118.62, 115.02, 110.70, 107.51, 98.87, 59.46, 51.57, 50.54, 49.38, 47.60, 14.76, 13.52. HRMS (ESI) m/z $[C_{29}H_{29}BF_2N_5O_2+H]^+$ calcd.: 528.2382, found: 528.2352.

THQ-BF₂-H: Dark red solid. Yield: 6.11%. ¹H NMR (400 MHz, CDCl₃) δ 9.69 (s, 1H), 7.93 (d, J = 7.5 Hz, 1H), 7.84 (d, J = 7.6 Hz, 1H), 7.55 (d, J = 9.0 Hz, 1H), 7.41 (p, J = 7.1 Hz, 3H), 7.18-7.03 (m, 2H), 6.78 (s, 2H), 6.26 (s, 1H), 3.94 (s, 3H), 3.71-3.56 (m, 2H), 3.45 (dq, J = 14.4, 7.2 Hz, 4H), 3.36-3.25 (m, 2H), 1.26 (dd, J = 12.3, 5.1 Hz, 6H). ¹³C NMR (100 MHz, CDCl₃) δ

159.31, 150.33, 145.07, 143.24, 141.53, 134.59, 133.33, 128.95, 128.09, 125.00, 124.41, 115.01, 114.79, 114.73, 111.10, 106.99, 94.96, 77.38, 77.26, 77.06, 76.74, 55.58, 49.92, 49.70, 49.49, 49.28, 49.06, 47.66, 46.62, 45.48, 43.67, 10.89, 9.72. HRMS (ESI) m/z [$C_{28}H_{26}BF_2N_5O_2+H$]⁺ calcd.: 498.2277, found: 498.2331.

THQ-BF₂-I: Dark red solid. Yield: 6.48%. ¹H NMR (500 MHz, DMSO-*d*₆) δ 7.93 (d, J = 8.5 Hz, 2H), 7.64 (d, J = 7.7 Hz, 1H), 7.52 (d, J = 7.6 Hz, 1H), 7.38 (d, J = 8.4 Hz, 2H), 7.18 (dt, J = 15.9, 6.8 Hz, 2H), 7.07 (s, 1H), 6.38 (s, 1H), 5.77 (s, 1H), 3.63-3.54 (m, 2H), 3.48 (q, J = 7.0 Hz, 2H), 3.41 (q, J = 7.0 Hz, 2H), 3.26 (t, J = 4.9 Hz, 2H), 1.25-1.12 (m, 3H), 1.09 (t, J = 7.1 Hz, 3H). ¹³C NMR (100 MHz, CDCl₃) δ 153.9, 147.9, 143.7, 142.5, 138.6, 133.1, 129.8, 127.2, 118.16, 115.6, 110.3, 103.8, 101.6, 99.9, 98.8, 94.5, 88.36, 51.4, 50.4, 49.4, 47.9, 14.6, 13.7. HRMS (ESI) m/z [$C_{28}H_{25}BF_2IN_5O+H$]⁺ calcd.: 624.1243, found: 624.1165.

2.3 Cell and zebrafish culture and fluorescence imaging

HeLa cells were used for imaging and toxicity experiments. HeLa cells were cultured using DMEM (GIBCO, Invitrogen) medium with 10% fetal bovine and 1% dual antibody (streptomycin and penicillin) at 37 °C in a humidified 5% CO₂ incubator. When the number of adherent cells grow steadily in the culture bottle reaches 85-95%, the digestion is passed on. Discard the original culture medium, wash the adhered cells three times with phosphate buffer solution (PBS), add trypsin to digest the cells for three minutes, and then add culture medium containing 10% serum to stop digestion. The digested cell suspension was transferred to the centrifugal tube for centrifugation (800 r/min, 3min), the supernatant was discarded, and cells were suspended and precipitated by a mixture of serum and dual antibody media. The cell concentration (about 2*10⁵ cells/mL) was adjusted and transferred to 96 orifice plate and co-focusing plate for MTT and bioimaging experiment, respectively.

Zebrafish was cultured at 28 °C in E3 embryo media, consisting of 15 mM NaCl, 0.5 mM MgSO₄, 1 mM CaCl₂, 0.15 mM KH₂PO₄, 0.05 mM Na₂HPO₄, 0.7 mM NaHCO₃ and 1% methylene blue, whose pH = 7.5. Three-day old zebrafish was selected for the imaging experiments.

3. Results and discussion

3.1 Photophysical properties in various solvents

With these dyes in hands, we firstly investigated their photophysical property in solutions (DCM, EtOH, CH₃CN and DMSO). **DEA-BF₂-R** dyes absorbed in a range from 482 nm to 497 nm with large molar extinction coefficients (about 10⁴ L*mol⁻¹cm⁻¹) and displayed green fluorescence with maxima ranging from 520 nm to 550 nm (Table 1 and Figures S1-S4). Compared with **DEA-BF₂-R**, **Julo-BF₂-R** displayed about 20 nm red-shift in their absorption spectra and 10 nm red-shift in emission spectra (shown in Table 1 and Figures S5-S8). We were very pleased that the replacement of diethylamino group with THQ group in borate dyes

significantly extended the emission to red spectral region (around 90 nm red shift) and resulted in about 40 nm red shift in their absorption spectra (Table 1 and Figures S9-S12). For example, the absorption maxima of **DEA-BF₂-CH₃** and **THQ-BF₂-CH₃** in DMSO were 483 nm and 526 nm and their fluorescence spectra peaked at 548 nm and 646 nm, respectively (shown in Figure 1). The Stokes shift for **THQ-BF₂-CH₃** was remarkably increased to 120 nm. As a result, we successfully tuned the optical properties of iminocoumarin-based borate complexes to obtain long-wavelength emission (> 600 nm) as well as large Stokes shift (>100 nm) through introducing THQ electron donor to enhance intracellular charge ICT process.

Table 1 Photophysical properties of **DEA-BF₂-R**, **Julo-BF₂-R** and **THQ-BF₂-R** in various solvents.

-R	Solvents	DEA-BF ₂ -R						Julo-BF ₂ -R						THQ-BF ₂ -R					
		$\lambda_{\text{abs}}/\lambda_{\text{em}}/\text{nm}$	$\Delta_{\text{ss}}/\text{nm}$	$\epsilon/\text{M}^{-1}\text{cm}^{-1}$	$\Phi_{\text{f}}^{\text{a}}$	τ/ns	X ^c	$\lambda_{\text{abs}}/\lambda_{\text{em}}/\text{nm}$	$\Delta_{\text{ss}}/\text{nm}$	$\epsilon/\text{M}^{-1}\text{cm}^{-1}$	$\Phi_{\text{f}}^{\text{a}}$	τ/ns	X ^c	$\lambda_{\text{abs}}/\lambda_{\text{em}}/\text{nm}$	$\Delta_{\text{ss}}/\text{nm}$	$\epsilon/\text{M}^{-1}\text{cm}^{-1}$	$\Phi_{\text{f}}^{\text{b}}$	τ/ns	X ^c
-CH ₃	DCM	490/525	35	41300	0.84	4.09	1.32	512/540	28	86500	0.79	4.19	1.25	534/607	73	31600	0.76	5.38	1.37
	EtOH	487/534	47	31300	0.77	3.82	1.20	507/545	38	31300	0.71	4.28	1.03	527/620	93	34000	0.44	4.05	1.22
	CH ₃ CN	483/537	54	34400	0.70	4.03	1.13	505/555	50	53300	0.69	4.43	1.24	522/626	104	30900	0.40	3.98	1.05
	DMSO	483/548	65	33000	0.72	3.53	1.34	505/559	54	53100	0.70	4.17	1.31	526/646	120	34400	0.29	3.11	1.11
-OCH ₃	DCM	493/531	38	42700	0.18	0.92	1.19	513/539	26	69800	0.65	3.54	1.08	538/610	72	24400	0.72	5.35	1.15
	EtOH	485/535	50	43900	0.11	0.63	1.38	505/546	41	39900	0.50	3.20	1.15	527/619	92	22300	0.46	4.15	1.07
	CH ₃ CN	484/537	53	41600	0.09	0.98	1.20	505/555	50	48500	0.60	3.92	1.03	521/626	105	21300	0.42	4.11	1.09
	DMSO	483/548	65	37400	0.24	1.35	1.19	505/559	54	38500	0.57	3.84	1.27	526/643	117	21700	0.32	3.29	1.02
-H	DCM	493/528	35	39300	0.84	4.20	1.02	513/538	26	63000	0.80	4.20	1.15	538/608	70	28800	0.75	5.35	1.29
	EtOH	488/534	46	34300	0.81	4.01	1.17	506/545	39	35600	0.73	4.25	1.04	528/621	93	24700	0.40	3.94	1.08
	CH ₃ CN	482/536	54	36300	0.73	4.09	1.11	505/554	39	37900	0.67	4.48	1.31	525/627	102	25900	0.39	3.85	1.14
	DMSO	482/547	65	31700	0.71	3.51	1.09	505/558	53	37700	0.65	4.15	1.47	528/650	122	26600	0.28	2.92	1.12
-I	DCM	497/532	35	34300	0.87	4.34	1.32	514/541	27	69200	0.84	4.45	1.22	537/611	74	40900	0.66	5.37	1.21
	EtOH	490/540	50	33000	0.83	4.12	1.33	508/550	42	18400	0.83	4.47	1.59	532/626	94	37600	0.37	3.77	1.03
	CH ₃ CN	486/542	56	34800	0.73	4.29	1.29	507/559	52	37700	0.69	4.68	1.24	532/632	100	41600	0.36	3.69	0.95
	DMSO	486/554	68	29500	0.71	3.61	1.26	508/564	56	38900	0.64	4.33	1.23	530/648	118	35200	0.16	2.80	1.46

^a Φ_{f} is the relative fluorescent quantum yield determined by using fluorescein as the reference ($\Phi = 0.92$ in 0.1 M NaOH at 25 °C). [31]

^b Φ_{f} is the relative fluorescent quantum yield determined using **Julo-BF₂-CH₃** as the reference ($\Phi = 0.79$ in DCM at 25 °C).

^c X is the linear fitting coefficient of the fluorescent lifetime.

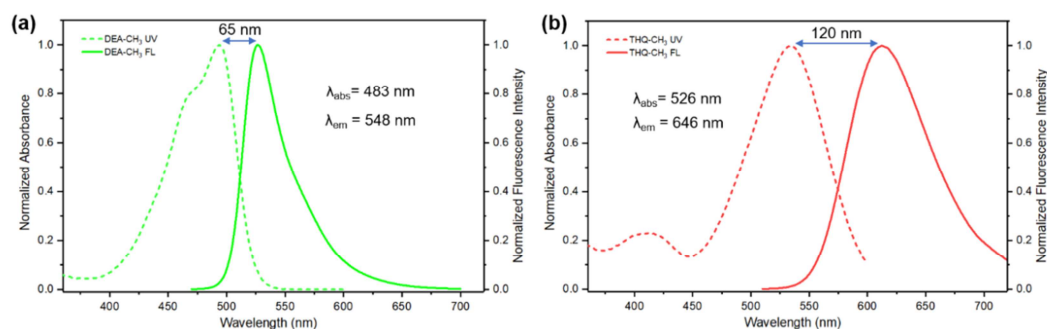


Figure 1. Normalized absorbance and fluorescence spectra of dyes (a) **DEA-BF₂-CH₃** and (b) **THQ-BF₂-CH₃** in DMSO.

As seen in Table 1, these iminocoumarin-based borate complexes exhibited relatively high fluorescent quantum yields in solutions. For **DEA-BF₂-R**, the fluorescent quantum yields were up to 0.7 and their fluorescent lifetimes are around 4.0 ns. However, there was an exception for **DEA-BF₂-OCH₃**, which was weakly fluorescent ($\Phi_f = 0.11$, $\tau = 0.63$ ns in EtOH). Similar to **DEA-BF₂-R**, **Julo-BF₂-R** exhibited high fluorescent quantum yields and long lifetimes. It's interesting that **Julo-BF₂-OCH₃** was much more fluorescent than **DEA-BF₂-OCH₃**. In particular, we were very pleased that red-emitting **THQ-BF₂-R** dyes were strongly fluorescent, especially in DCM ($\Phi_f = 0.66$ - 0.76), and their fluorescent quantum yields were up to 0.4 even in polar solution, which should be ascribed to the rigidity of THQ moiety. It's noted that **THQ-BF₂-OCH₃** displayed a similar fluorescent quantum yield to other **THQ-BF₂-R** dyes.

In addition, a bathochromic shift in the emission spectra and a decrease in the fluorescent quantum yields were observed for **THQ-BF₂-R** dyes with increasing polarity of the solvents. For instance, when the solvents went from DCM, EtOH, CH₃CN to DMSO, **THQ-BF₂-CH₃** exhibited red-shifts in their emissions from 607 nm, 620 nm, 626 nm to 646 nm whereas the fluorescent quantum yields dropped from 0.76, 0.44, 0.40 to 0.29. The same phenomena were observed in the optical properties of **DEA-BF₂-R** and **Julo-BF₂-R** dyes. Moreover, when **DEA-BF₂-CH₃**, **Julo-BF₂-CH₃** and **THQ-BF₂-CH₃** were irradiated in acetonitrile under a 500 W Xe-lamp light, all the dyes can keep 80% absorption strength after 80 min of radiation, indicating the good photostability, as shown in Figure S13.

3.2 Theoretical calculations

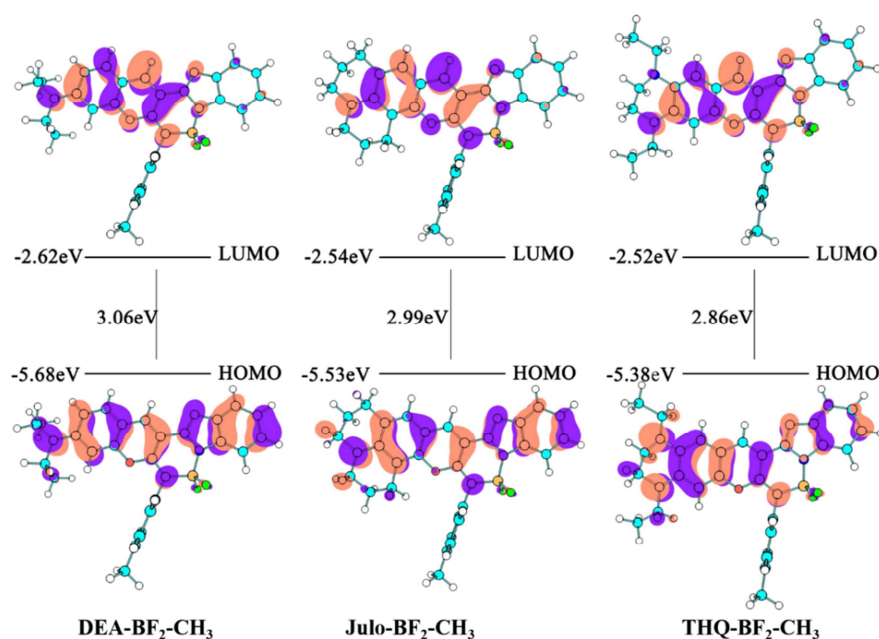


Figure 2. Molecular orbital plots (LUMO and HOMO) and HOMO/LUMO energy gaps of **DEA-BF₂-CH₃**, **Julo-BF₂-CH₃** and **THQ-BF₂-CH₃** in DCM solvent.

To obtain more evidence to support our design strategy, DFT calculations were performed on **DEA-BF₂-CH₃**, **Julo-BF₂-CH₃** and **THQ-BF₂-CH₃** using Gaussian 09 program, whose geometries were optimized under B3LYP/6-31G level, and the frontier energy levels (HOMO and LUMO) were calculated in DCM solvent. As depicted in Figure 2, the π electrons of the HOMO of **DEA-BF₂-CH₃** were mainly located on the coumarin core, N, N-diethyl donor and benzimidazole moiety. At the excited state, the electron clouds were mostly located on coumarin core and BF₂ bridge linking iminocoumarin core. For **DEA-BF₂-CH₃**, **Julo-BF₂-CH₃** and **THQ-BF₂-CH₃**, the energy gaps between HOMOs and LUMOs decreased (from 3.06 eV, 2.99 eV to 2.86 eV) owing to the enhanced conjugation of donors (Julo and THQ) to iminocoumarin-BF₂ framework, which was well in agreement with the red-shift in their absorption wavelength.

3.3 Solid fluorescence

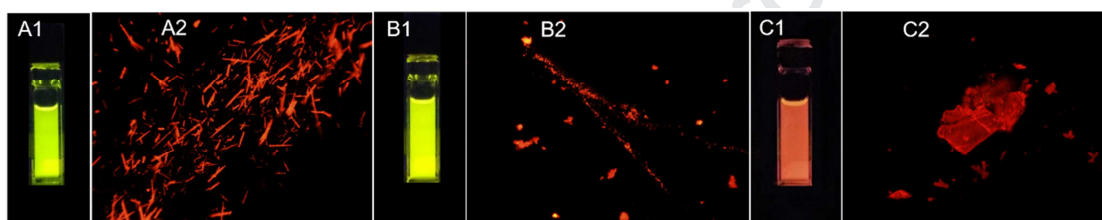


Figure 3. Photographs of (A) **DEA-BF₂-CH₃**, (B) **Julo-BF₂-CH₃** and (C) **THQ-BF₂-CH₃** (1) in a solution of DCM under UV-bench lamp ($\lambda_{\text{ex}} = 365 \text{ nm}$), (2) in solid state under 10 \times fluorescence inverse microscope.

Table 2 Photo-physical property of **DEA-BF₂-R**, **Julo-BF₂-R** and **THQ-BF₂-R** in solid state.

Dyes	$\lambda_{\text{em}} / \text{nm}$	Φ_f	τ / ns	X
DEA-BF₂-CH₃	634	0.08	4.95	1.47
DEA-BF₂-OCH₃	608	0.08	4.27	1.47
DEA-BF₂-H	604	0.07	3.43	1.42
DEA-BF₂-I	614	0.10	5.75	1.19
Julo-BF₂-CH₃	624	0.02	1.08	1.32
Julo-BF₂-OCH₃	622	0.01	1.36	1.22
Julo-BF₂-H	635	0.01	0.95	1.08
Julo-BF₂-I	636	0.02	1.16	1.41
THQ-BF₂-CH₃	713	0.01	0.81	1.54
THQ-BF₂-OCH₃	665	0.01	0.39	1.38
THQ-BF₂-H	666	0.01	0.82	1.23
THQ-BF₂-I	719	0.01	0.97	0.86

Next, the solid fluorescence of these borate dyes was investigated. **DEA-BF₂-R**, **Julo-BF₂-R** and **THQ-BF₂-R** all exhibited strong red solid fluorescence. As shown in Figure 3, **DEA-BF₂-CH₃**, **Julo-BF₂-CH₃** and **THQ-BF₂-CH₃** at solid state showed different

crystalline morphologies. The emission spectra, fluorescent quantum yields (Φ_f) and lifetimes (τ) of all three kinds of dyes were summarized in Table 2 and Figure S14. The emission wavelength of these dyes increased in an order of **DEA-BF₂-R**, **Julo-BF₂-R** and **THQ-BF₂-R** and their fluorescent quantum yields and fluorescent lifetimes dropped in the same order. it's noteworthy that **THQ-BF₂-CH₃** and **THQ-BF₂-I** had emissions in near-infrared spectra region ($\lambda_{\max}^{\text{Em}} = 713$ and 717 nm, respectively). The solid-state fluorescence might be ascribed to the existence of twisted 3D structure in these dyes, which could prevent π - π stacking interactions.[12, 32]

3.4 Cell and zebrafish imaging

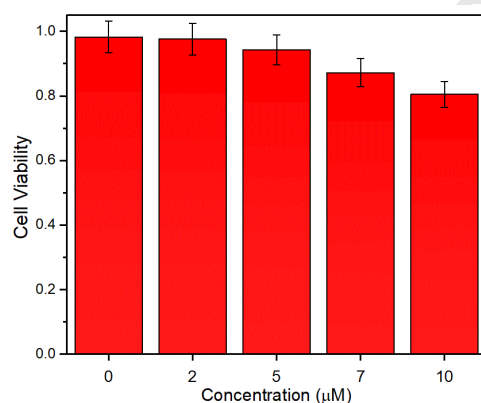


Figure 4. Cytotoxicity assay of **THQ-BF₂-CH₃** at different concentrations in HeLa cells.

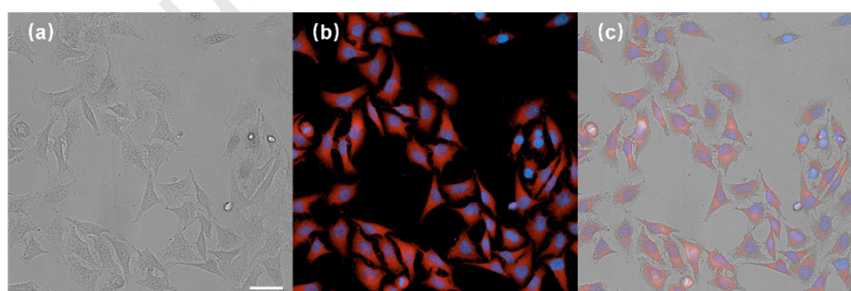


Figure 5. High content screening images of HeLa cells after incubation with dye **THQ-BF₂-CH₃** ($2.0 \mu\text{M}$) and Hoechst 33342 ($1.0 \mu\text{M}$) for 15 min, respectively, at 37°C . Red channel: **THQ-BF₂-CH₃**: $\lambda_{\text{ex}} = 490\text{-}515$ nm, $\lambda_{\text{em}} = 570\text{-}650$ nm; Blue channel: Hoechst 33342: $\lambda_{\text{ex}} = 350$ nm, $\lambda_{\text{em}} = 430\text{-}500$ nm. (a) Bright field, (b) merged of red channel and blue channel, (c) overlay of bright field and dark field. Scale bar: $50 \mu\text{m}$.

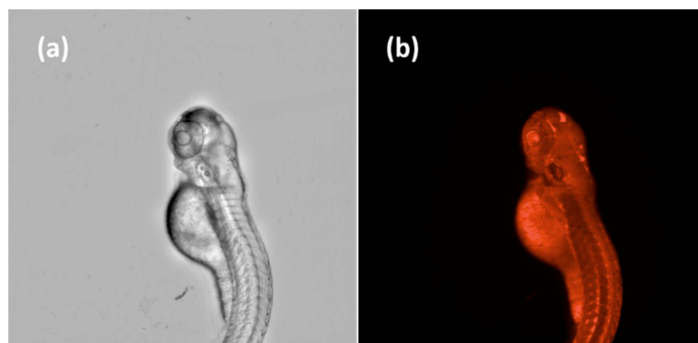


Figure 6. High content screening images of zebrafish after incubation with dye **THQ-BF₂-CH₃** (2.0 μ M) for 20 min at 28 °C. (a) Bright field; (b) Red channel: **THQ-BF₂-CH₃**; λ_{ex} = 490-515 nm, λ_{em} = 570-650 nm.

The excellent optical properties of these dyes encouraged us to explore their applications for bioimaging. First, we evaluated the cytotoxicity of **THQ-BF₂-CH₃** by MTT assays. As shown in Figure 4, the cell viabilities were over 94% when cells were incubated with **THQ-BF₂-CH₃** at a concentration below 5.0 μ M, indicating the low cytotoxicity of dye **THQ-BF₂-CH₃**. Then, we used **THQ-BF₂-CH₃** to image living HeLa cells co-stained with Hoechst 33342 (nucleus indicator). When cells were incubated with **THQ-BF₂-CH₃** for 15 min, strong red fluorescence was viewed from cytoplasm (shown in Figure 5). Furthermore, we fed a 3-day-old zebrafish with **THQ-BF₂-CH₃** for 20 min at 28 °C and remarkable red fluorescence was observed (shown in Figure 6). The imaging experiments in cells and zebrafish suggested **THQ-BF₂-R** dyes were cell-membrane penetrable and could be used as staining agents for biological applications.

4. Conclusions

In conclusion, we developed a series of borate fluorescent dyes, **THQ-BF₂-R**, using tetra-hydro-quinoxaline as the electron donor, which displayed large Stokes shifts, red emissions and fairly high fluorescent quantum yields in solution, as well as exhibited red/NIR solid fluorescence and could stain living cells and zebrafish with good performance and low cytotoxicity.

Acknowledgements

This work was supported by the National Natural Science Foundation of China (No. U1608222), the State Key Laboratory of Fine Chemicals (KF1606), the State Key Laboratory

of Chemo/Biosensing and Chemometrics (2016005), Special Fund for Agro-scientific Research in the Public Interest of China (No. 201503108) and the Fundamental Research Funds for the Central Universities of Central South University (No. 2019zzts002 and No. 2019zzts438).

References

- [1] Kowada T, Maeda H, Kikuchi K. BODIPY-based probes for the fluorescence imaging of biomolecules in living cells. *Chemical Society Reviews*. 2015;44(14):4953-72.
- [2] Boens N, Leen V, Dehaen W. Fluorescent indicators based on BODIPY. *Chemical Society Reviews*. 2012;41(3):1130-72.
- [3] Yue Y, Huo F, Cheng F, Zhu X, Mafireyi T, Strongin RM, et al. Functional synthetic probes for selective targeting and multi-analyte detection and imaging. *Chemical Society Reviews*. 2019;48(15):4155-77.
- [4] Xu M, Kelley SP, Glass TE. A Multi-Component Sensor System for Detection of Amphiphilic Compounds. *Angewandte Chemie-International Edition*. 2018;57(39):12741-4.
- [5] Zhang L, Liu XA, Gillis KD, Glass TE. A High-Affinity Fluorescent Sensor for Catecholamine: Application to Monitoring Norepinephrine Exocytosis. *Angewandte Chemie-International Edition*. 2019;58(23):7611-4.
- [6] Kamkaew A, Lim SH, Lee HB, Kiew LV, Chung LY, Burgess K. BODIPY dyes in photodynamic therapy. *Chemical Society Reviews*. 2013;42(1):77-88.
- [7] Benniston AC, Copley G. Lighting the way ahead with boron dipyrromethene (Bodipy) dyes. *Physical Chemistry Chemical Physics*. 2009;11(21):4124-31.
- [8] Bessette A, Hanan GS. Design, synthesis and photophysical studies of dipyrromethene-based materials: insights into their applications in organic photovoltaic

- devices. *Chemical Society Reviews*. 2014;43(10):3342-405.
- [9] Loudet A, Burgess K. BODIPY dyes and their derivatives: Syntheses and spectroscopic properties. *Chemical Reviews*. 2007;107(11):4891-932.
- [10] Ulrich G, Ziessel R, Harriman A. The chemistry of fluorescent bodipy dyes: Versatility unsurpassed. *Angewandte Chemie-International Edition*. 2008;47(7):1184-201.
- [11] Hong Y, Lam JWY, Tang BZ. Aggregation-induced emission. *Chemical Society Reviews*. 2011;40(11):5361-88.
- [12] Mei J, Leung NL, Kwok RT, Lam JW, Tang BZ. Aggregation-Induced Emission: Together We Shine, United We Soar! *Chemical Reviews*. 2015;115(21):11718-940.
- [13] Araneda JF, Piers WE, Heyne B, Parvez M, McDonald R. High Stokes shift anilido-pyridine boron difluoride dyes. *Angewandte Chemie-International Edition*. 2011;50(51):12214-7.
- [14] Frath D, Massue J, Ulrich G, Ziessel R. Luminescent Materials: Locking pi-Conjugated and Heterocyclic Ligands with Boron(III). *Angewandte Chemie-International Edition*. 2014;53(9):2290-310.
- [15] Frath D, Poirel A, Ulrich G, De Nicola A, Ziessel R. Fluorescent boron(III) iminocoumarins (Boricos). *Chemical Communications*. 2013;49(43):4908-10.
- [16] Peng XJ, Song FL, Lu E, Wang YN, Zhou W, Fan JL, et al. Heptamethine cyanine dyes with a large stokes shift and strong fluorescence: A paradigm for excited-state intramolecular charge transfer. *Journal of the American Chemical Society*. 2005;127(12):4170-1.
- [17] Liu J, Sun YQ, Zhang H, Shi H, Shi Y, Guo W. Sulfone-Rhodamines: A New Class of Near-Infrared Fluorescent Dyes for Bioimaging. *ACS applied materials & interfaces*.

2016;8(35):22953-62.

[18] Yuan L, Lin W, Chen H. Analogs of Changsha near-infrared dyes with large Stokes Shifts for bioimaging. *Biomaterials*. 2013;34(37):9566-71.

[19] Xiong K, Huo F, Chao J, Zhang Y, Yin C. Colorimetric and NIR Fluorescence Probe with Multiple Binding Sites for Distinguishing Detection of Cys/Hcy and GSH in Vivo. *Analytical Chemistry*. 2019;91(2):1472-8.

[20] Zhang W, Huo F, Zhang Y, Yin C. Dual-site functionalized NIR fluorescent material for a discriminative concentration-dependent response to SO₂ in cells and mice. *Journal of Materials Chemistry B*. 2019;7(11):1945-50.

[21] Zhang W, Huo F, Yin C. Photocontrolled Single-/Dual-Site Alternative Fluorescence Probes Distinguishing Detection of H₂S/SO₂ in Vivo. *Organic Letters*. 2019;21(13):5277-80.

[22] Hou P, Chen S, Wang H, Wang J, Voitchovsky K, Song X. An aqueous red emitting fluorescent fluoride sensing probe exhibiting a large Stokes shift and its application in cell imaging. *Chemical Communications*. 2014;50(3):320-2.

[23] Ren TB, Xu W, Zhang W, Zhang XX, Wang ZY, Xiang Z, et al. A general method To increase Stokes shift by introducing alternating vibronic structures. *Journal of the American Chemical Society*. 2018;140(24):7716-22.

[24] Liu X, Li Y, Ren X, Yang Q, Su Y, He L, et al. Methylated chromenoquinoline dyes: synthesis, optical properties, and application for mitochondrial labeling. *Chemical Communications*. 2018;54(12):1509-12.

[25] Geng Y, Tian H, Yang L, Liu X, Song X. An aqueous methylated chromenoquinoline-based fluorescent probe for instantaneous sensing of thiophenol with a red

emission and a large Stokes shift. *Sensors and Actuators B-chemical*. 2018;273:1670-5.

[26] Liu X, Cole JM, Xu Z. Substantial Intramolecular Charge Transfer Induces Long Emission Wavelengths and Mega Stokes Shifts in 6-Aminocoumarins. *Journal of Physical Chemistry C*. 2017;121(24):13274-9.

[27] Chen W, Xu S, Day JJ, Wang DF, Xian M. A General Strategy for Development of Near-Infrared Fluorescent Probes for Bioimaging. *Angewandte Chemie-International Edition*. 2017;56(52):16611-5.

[28] Grabowski ZR, Rotkiewicz K, Rettig W. Structural changes accompanying intramolecular electron transfer: focus on twisted intramolecular charge-transfer states and structures. *Chemical reviews*. 2003;103(10):3899-4032.

[29] Liu X, Qiao Q, Tian W, Liu W, Chen J, Lang MJ, et al. Aziridiny Fluorophores Demonstrate Bright Fluorescence and Superior Photostability by Effectively Inhibiting Twisted Intramolecular Charge Transfer. *Journal of the American Chemical Society*. 2016;138(22):6960-3.

[30] Rajagopal R, Shenoy VU, Padmanabhan S, Sequeira S, Seshadri S. Synthesis of fluorescent 2, 3-fused coumarin derivatives. *Dyes and Pigments*. 1990;13(3):167-75.

[31] Weber G, Teale FWJ. Determination of the absolute quantum yield of fluorescent solutions. *Transactions of the Faraday Society*. 1957;53:646.

[32] Luo J, Xie Z, Lam JWY, Cheng L, Tang BZ, Chen H, et al. Aggregation-induced emission of 1-methyl-1,2,3,4,5-pentaphenylsilole. *Chemical Communications*. 2001;18(18):1740-1.

Highlights

1. A series of new iminocoumarin-based fluorescent borate complexes was developed by introducing a very strong electron donor, tetrahydroquinoline group.
2. These dyes displayed red/NIR emissions (up to 650 nm in DMSO) and large Stokes shift (up to 122 nm in DMSO).
3. These dyes had good fluorescent quantum yields (0.65-0.84 in DCM) and large absorption molecular extinction coefficients ($10^4 \text{ M}^{-1}\text{cm}^{-1}$).
4. These dyes showed red/NIR solid fluorescence.
5. These dyes had potential application for bioimaging in cells and zebrafish.

Declaration of interests

The authors declare that they have no known competing financial interests or personal relationships that could have appeared to influence the work reported in this paper.

The authors declare the following financial interests/personal relationships which may be considered as potential competing interests:

Journal Pre-proof